TT-TRITIUM BREEDING AND MATERIALS
TTMI – IFMIF

TASK: TW5-TTMI-003
IFMIF, TEST FACILITIES

***Deliverables*: X-ray microtomography for HFTM capsules and rigs: (i) influence of the sample radioactivity on the tomographic reconstruction quality and practical procedures to mitigate its effects, and (ii) experimental determination of resolution limits of specimens, capsules and rig assemblies**

I. Tiseanu, T. Craciunescu, N.B.Mandache, F. Gherendi

National Institute for Laser, Plasma and Radiation Physics, Bucharest-Magurele

1. Introduction

Presently the X-ray micro-tomography is the only reliable solution for official inspections of the structural integrity of IFMIF (International Fusion Materials Irradiation Facility) complete assemblies before, during and after irradiation campaigns [1]. Hence the successful demonstration of micro-tomography on the assembled irradiation capsule is crucial. We determined through a hard way using a real capsule, the limit of the current technology, in observing any flaws in the testing samples and capsule itself. The space resolution achieved in these measurements allows us to assess the loading quality of the capsule and even determines the 3-D positioning of the capsule components down to couple of tens of microns. Finally, the reconstructed volume can serve as a 3-D model of the "as manufactured" instrumented capsule to be used as input in thermal hydraulics and stress analysis codes.

The qualification of structural materials in a future fusion reactor requires long-term irradiation in fusion-relevant neutron spectra leading to material damages of up to 150 dpa. IFMIF promises to satisfy the requirements of fusion-relevant material tests regarding the parameters irradiation damage, test volume and neutron flux. The main challenge to the well established transmission microtomography inspection is the influence of the sample radioactivity (produced by neutron activation) on the tomographic reconstruction quality. The goal of this study was the evaluation of this influence. As far as we know the present report is one of the first approaches on this topic. It has been carried out by 3D Monte Carlo radiation transport simulations corroborated with previous extensive tomographic measurements on HFTM irradiation capsules. After assessing the level of perturbation induces by the sample radioactivity we propose practical procedures to mitigate its effects.

2. X-ray tomography of the irradiation capsules

In order to identify the optimum irradiation parameters and scanning configuration we carried out a comparative NDT analysis on two micro-tomography facilities, our compact, high magnification installation at NILPRP [2] and two high-end industrial tomography facilities

with higher X-ray energy and intensity. The study was performed in cooperation with Hans Wälischmiller (HWM) Institute from Germany [3]. The main difference consists in the energy and intensity of the X-ray output. We investigated the irradiation capsule for the High Flux Test Module manufactured by FZ Karlsruhe. We report here the CT results obtained in similar conditions for spatial sampling (voxel size 50-65 μm).

Taking into account the overall dimension of the HTFM irradiation capsule, the first experiment was performed using high X-ray energy in order to ensure a high penetrability. Significant results are presented in Figure 1. One can observe that an overall description of the capsule structure can be obtained. However high energy implies a large focus spots and, consequently, lower resolution in the reconstruction. This impedes the visualization of fine details of specimens inside the irradiation capsule.

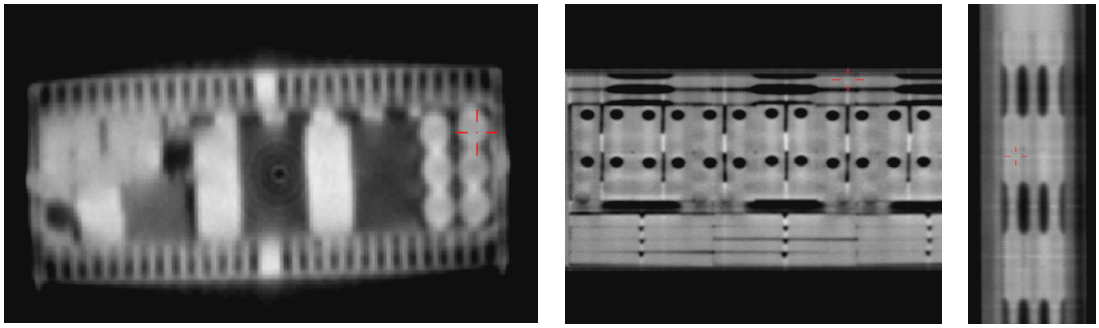

Figure 1. Cross-sections through the 3D tomographic reconstruction of the HFTM irradiation capsule obtained at high energy (U=450 kV).

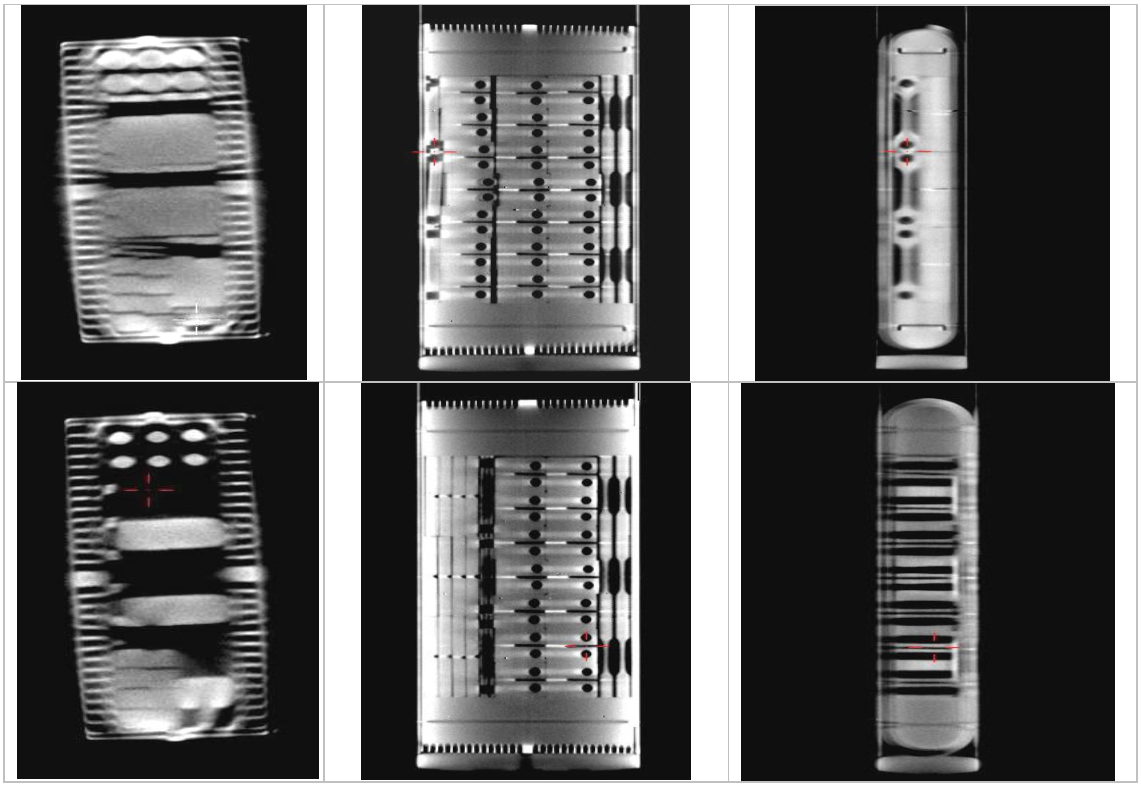

Figure 2. Cross-sections of the 3D tomographic reconstruction of the HFTM irradiation capsule obtained for optimum combination of the irradiation parameters (High Voltage= 220 kV, X-ray tube current ~ 300 μA) with full object scanning geometry.

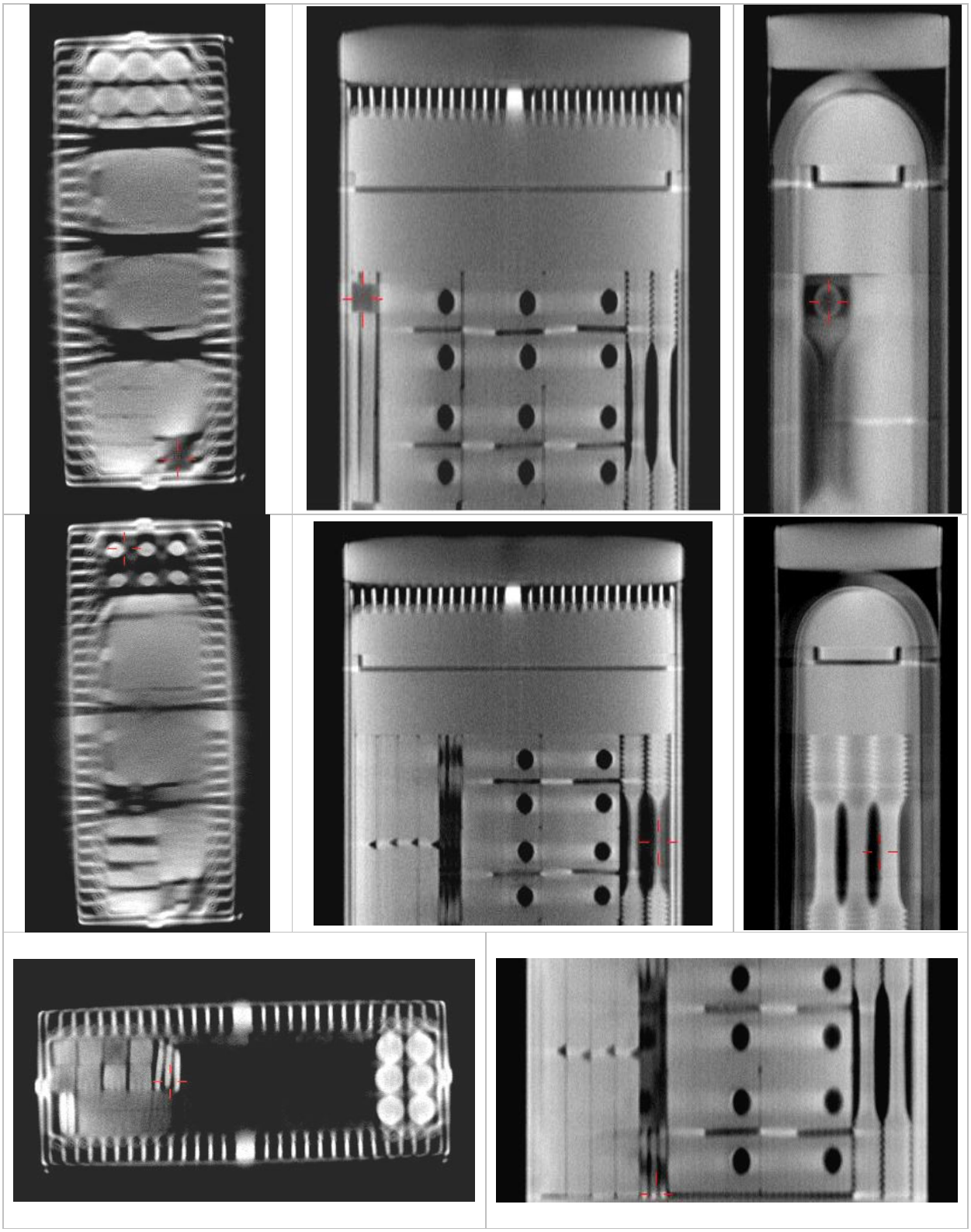

Figure 3. Tomographic reconstruction of the HFTM irradiation capsule obtained for optimum combination of the irradiation parameters (U = 220 kV, I = 300 μA.) with enhanced magnification for detail visualization.

Optimum results were obtained with a microfocus X-ray tube with following operational parameters: X-ray tube high voltage ~ 220 kV and X-ray tube current ~ 300 μA.

The high voltage ensures enough penetrability and the source current was chosen as a compromise between a good statistic in radiographic images and a good resolution (high source current means larger focus spots and, consequently, lower resolution in the radiographic image).

Significant results are presented in Figures 2÷4. The figure displays correlated axial, longitudinal and sagital cross-sections in order to facilitate object identification (the cross in each picture indicates the same point inside the object). Cross-sections through the 3D reconstructed object enable line profiling and accurate geometrical measurements, as illustrated in Figure 5. The achieved geometry resolution is about 30-50 microns for characteristic dimension up to 100 mm.

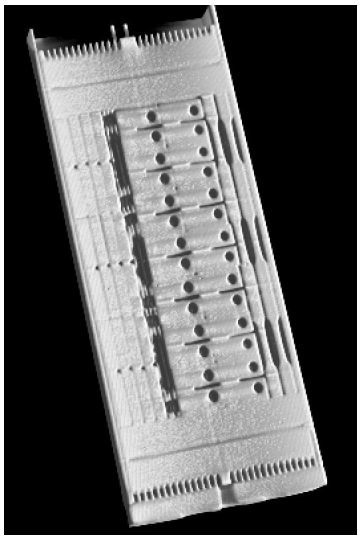

Figure 4. 3D reconstruction of the HFTM irradiation capsule

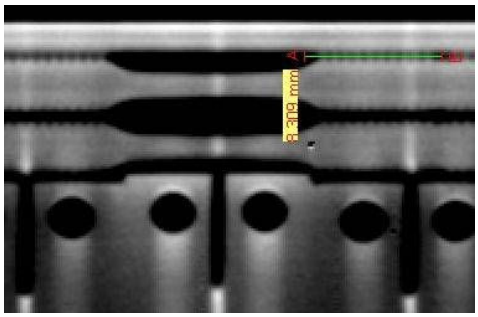

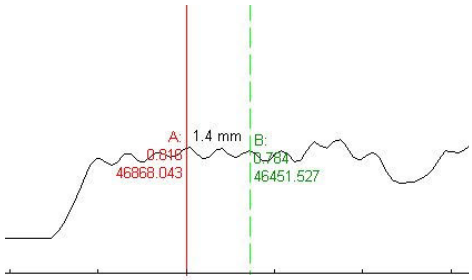

Figure 5. Cross-sections through 3D reconstructed object are used for line profiling and geometrical measurements

3. Beam hardening correction

As the HFTM irradiation capsule is a high density sample, beam hardening artifacts can be observed in the reconstruction. Beam hardening artifact consists of an elevated density displayed on the perimeter of a uniform density probe and a corresponding density depression in the probe's core region. It is caused by the polychromatic structure of the energy spectrum of the X-ray generators. As long as the beam hardening effect is not diminished the interpretation of the tomographic reconstructions are strongly impaired. That is true for mainly for quantitative analysis but even qualitative inspection tasks are complicated.

Several techniques were reported for beam-hardening correction both for pre-processing of the radiographic data and post-processing of the reconstructed arrays [4-6]. The former are considered most effective. Their goal is primarily the determination of the non-linear dependence between investigated object thickness and log ratio of intensities in the radiographic views, followed by the corresponding processing of the radiographic data.

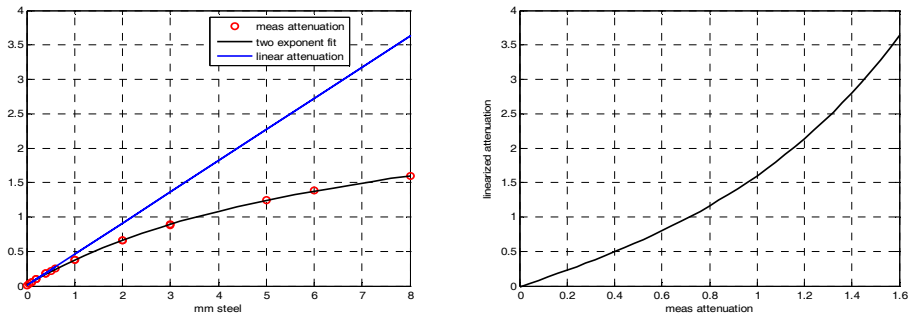

Figure 6 – Beam hardening correction: measured attenuation and linearized attenuation (left); correction curve to be used in the projection processing step of the reconstruction algorithm (right).

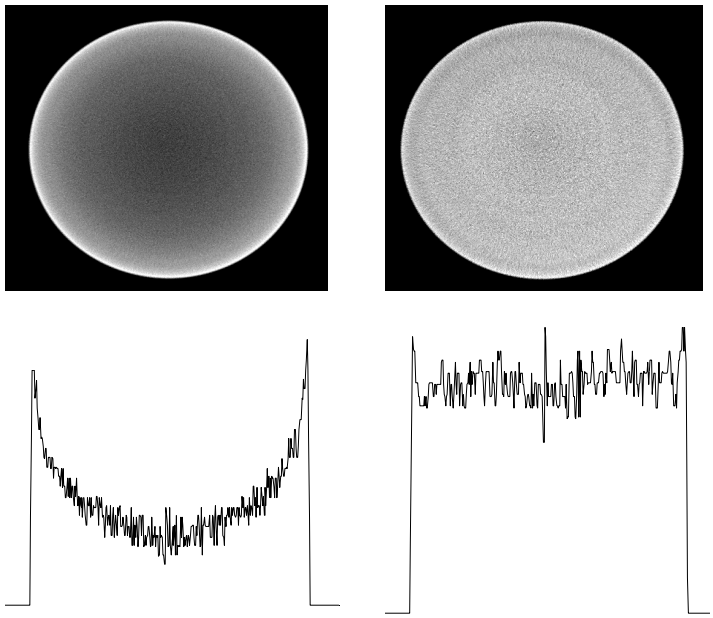

Figure 7 – Comparison of reconstructions of homogeneous steel cylinder without (left) and with (right) beam hardening correction.

Here we report the typical steps of the beam hardening correction technique by linearization of attenuation curve. Firstly, the attenuation curve was measured using a set of samples of different thicknesses. In our experiment we used stainless steel, most probably not same chemical composition as that of the HFTM capsule. In the future one need to obtain a set of plate samples of same alloy that is used in HFTM capsule manufacturing. Figure 6 shows the measured attenuations, the two-exponential fitting curve and the linearized attenuation curve (left) and the resulting correction curve that it is used the projection processing step of the reconstruction algorithm (right).

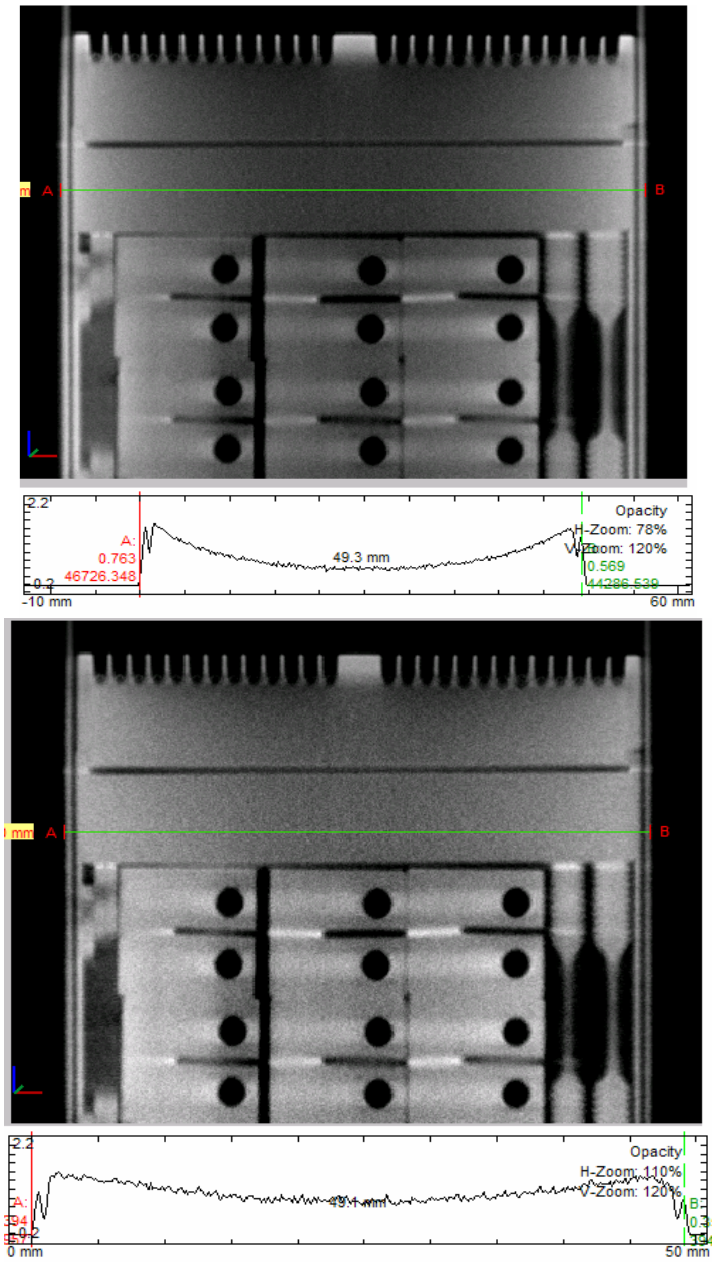

Figure 8 – Illustration of the efficiency of beam hardening artifact correction method. By applying the linearization correction of the absorption curve on the original image (up) one obtains a substantial reduction of the artifact (down).

Finally the result of application of this procedure is presented in Figure 7. As example of sample with strong beam hardening artifact we show the reconstruction of a stainless steel cylinder of 12.6 mm diameter. In a reconstruction that does not employs beam hardening correction procedure the horizontal profile displays a strong depression in the core region, although the body is made of homogeneous material. This effect is perfectly corrected in the reconstruction treated with the beam hardening correction procedure.

Figure 8 illustrates the application of the set of beam hardening coefficients obtained by the procedure described above to the reconstruction of the HFTM capsule. One can note that by applying the linearization correction of the attenuation curve on the original image one obtains a substantial reduction of the artifact. This result is very encouraging taking into account that we did not use same material and most significant the steel plates had thicknesses in the range 50 microns to only 8 mm, much less than the maximum radiation path through the HFTM capsule of up to 50 mm. In the future tests one needs to design and build an appropriate set of calibration samples in order to compensate the beam hardening artifacts.

Besides the beam hardening artifact, a treatment of the ring artifacts, inherent when using 2-D X-ray detectors, was performed. Ring artifacts are produced by parallel straight lines induced in projection images by the detector non-uniformity patterns that are transformed in circular ring pattern emanating from the central point by the back-projecting algorithm. We applied a method previously developed and implemented in order to remove the variation in grey-level as one proceeds from one radial distance to another, since it is this variation that is responsible for the observed ring pattern. Because of the concentric ring nature of this noise, a special filter function is applied in each plane each radial distance. This procedure can be applied iteratively. Alternatively, as the X-ray detector is mounted on a micrometric manipulator, random movement with the selected amplitude, given in a number of lines on the camera, was used as an efficient technique to reduce the ring artifacts in the reconstructed cross sections.

4. Influence of the sample radioactivity on the tomographic reconstruction quality and practical procedures to mitigate its effects

An inspection procedure to assess the mechanical integrity of IFMIF capsules and rigs during the irradiation campaign is necessary. The main challenge to the well established transmission microtomography inspection is the influence of the sample radioactivity (induced by neutron activation) on the tomographic reconstruction quality.

For this assessment, a working environment able to provide a realistic numerical simulation of a tomographic measurement was established on the basis of the integrated TIGER series (ITS, Sandia National Laboratories) time-independent multimaterial and multidimensional-coupled electron/photon Monte Carlo transport code.

The average energy deposition in the tomography detection system was calculated for a typical sample with and without remanent gamma radioactivity. The ratio between energy deposition by X-ray and that by γ-ray was selected as most significant parameter to assess the influence of the sample radioactivity on the tomographic reconstruction quality.

A special interest must be paid for tokamak first wall radiation resistant, low activation steel alloys. Most relevant candidates are considered SS 316 and EUROFER 97 steel alloys. In our evaluation we considered the SS-316 inventory as being of a special interest for IFMIF experiments. For SS 316 and EUROFER 97 steel alloys and IFMIF neutron energy spectrum ^{51}Cr isotope with γ–ray at 320 keV and life time of 27.7 days has by far most significant specific activity in the context of months-years irradiation time and relatively short cooling periods (weeks-months**).** For a long irradiation time (one up to few years – typical for IFMIF experiments) experimental data are not published in the open literature. In our analysis we used the evaluation performed in FZK [7]. Figure 9 shows that for IFMIF neutron spectrum and intensity, the gamma activity – HFTM case - increases significantly especially due to ^{51}Cr up to specific saturation activity of about 1014 Bq/kg. One should note that isotopes as ^{55}Fe, ^{3}H, ^{14}C do not contribute to the gamma radioactivity.

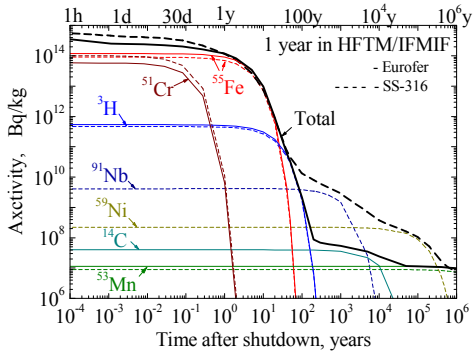

Figure 9. Total and specific isotope γ–ray activities induced in the Eurofer (solid lines) and SS-316 (dashed lines) steels after 1 year irradiation in the HFTM of the IFMIF.

In our evaluation we determined the energy deposition in the detector for the gamma line of 320 keV of ^{51}Cr after one life time (approximately one month) of cooling period. The ratio between energy deposition (X-ray/γ-ray), is presented in Table 1.

Table 1 – Ratio between energy depositions (X-ray/γ-ray)
HFTM – one year irradiation

	X-ray tube current (μA)			
X-ray tube High Voltage (kV)	100	300	500	1000
150	0.16	0.47	0.78	1.56
200	0.28	0.83	1.39	2.78
300	0.42	1.25	2.09	4.17

The most favorable energy deposition ratio is ensured by the parameters: HV=300 kV, I=1000 μA. However, high source current means larger focus spots and, consequently, lower resolution in the radiographic image. Therefore it is recommended to use same high voltage but lower current (I=300 μA). The result of the generated radiographies of the gamma radioactive sample is presented in Figure 10.

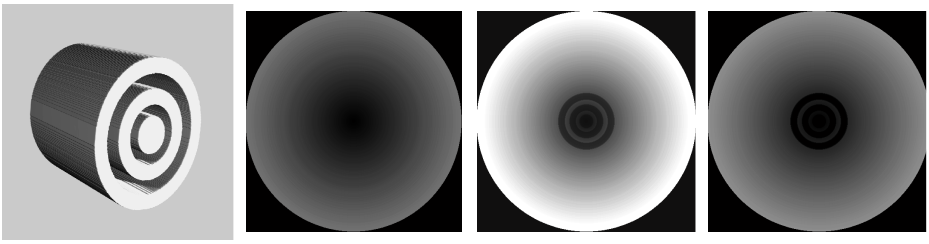

Figure 10. Investigated sample (left) and HFTM results (1 year irradiation): autoradiography showing the gamma ray influence on the detector (middle-left), X-ray radiography of the gamma radioactive sample (middle-right), X-ray radiography after subtracting the autoradiography (right).

The gamma radioactivity of the sample produces a smearing effect on the radiographies. The main influence of an intense gamma radioactivity, after subtraction, is the reduced dynamic range in the processed radiographies with the obvious consequence of increasingly noisy reconstructions. If the noise level in the reconstruction becomes unacceptable the high level gamma activity can be exploited and turned into advantage by using, for non-destructive examinations, the emission tomography.

Our group has previously [8] delivered a conceptual design of an emission tomography system established by numerical simulations and validated by experimental tests. The emission tomography reconstructions presented in that report show that the design parameters for space resolution and isotope selectivity are well within reach.

Finally, based on radioactivity estimation of various gamma-ray isotopes, corroborated with measured data, one has concluded that the components of the tomograph should be designed and fabricated to fully fulfill the working conditions in a hot cell environment.

5. Conclusion

An inspection procedure to assess the mechanical integrity of IFMIF capsules and rigs during the irradiation campaign is necessary. By extensive experiments we determined that for the currently measured capsule the geometry resolution is about 30-50 microns for characteristic dimension of 50 mm. We can guaranty this resolution up to sample size of characteristic dimension of 100 mm. Voids of 30 microns diameter and cracks of 30 microns width can be detected. The absolute error of geometrical measurements should be sufficient for the assessment of the structural integrity of the irradiation capsule and for the geometry description of the thermal-hydraulic modeling. Despite strong differences between HFTM and MFTM both as structure and composition the tomography results obtained during 2005 work are extendable for the assessment of structural integrity of the MFTM.

Previously developed methods for beam-hardening and ring artefacts correction were refined and used to obtain high quality tomographic reconstructions. Here we have presented a validation of these methods in HTFT tomographic examination conditions.

An inspection procedure to assess the mechanical integrity of IFMIF capsules and rigs during the irradiation campaign is necessary. The main challenge to the well established transmission microtomography inspection is the influence of the sample radioactivity

on the tomographic reconstruction quality. A special interest has been paid for tokamak first wall radiation resistant, low activation steel alloys as SS 316 and EUROFER 97.

We have found that the influence of the autoradiography on the X-ray image is relatively strong, typically amounting to half the average energy deposition in the tomography detection system, consequently, leading to degradation of reconstruction parameters (increasingly noisy reconstructions). If the noise level in the reconstruction becomes unacceptable the high level gamma activity can be exploited and turned into advantage by using, for non-destructive examinations, the emission tomography.

As far as we know the present report is one of the first approaches on this topic. Once the methodology was fully established, we believe that this study should be continued for the specific configuration of newly manufactured IFMIF irradiation capsules also incorporating the latest activation data.

6. Outlook

Recently FZ Karlsruhe has refined the HFTM rig design and manufacturing process and is going to fabricate fully equipped and instrumented irradiation rigs. In addition to the NDT task performed on the HFTM prototype in 2005 one would need to identify the NaK filling height and distribution in the specimen volume and, even more challenging, to asses the quality of the brazing material layer. Also, FZK needs a reliable method for the NDT investigation of the heater plates of the flat duct test-section of ITHEX. The overall "loading quality" and the structural integrity will be evaluated and various geometrical measurements will be performed. Finally, the reconstructed volume would serve as a 3-D model of the "as manufactured" instrumented capsule to be used as input in thermal hydraulics and stress analysis codes.

Another goal is to refine the newly proposed methodology for the simulation of the influence of the sample radioactivity (induced by neutron activation) on the tomographic reconstruction quality and to propose practical procedures to mitigate its effects. Latest activation data will be incorporated.

References

[1] ***, "*IFMIF Comprehensive Report Design"* 2003

[2] **Tiseanu I., Craciunescu T., Mandache N. B.**, *"Non-destructive analysis of miniaturized samples and irradiation capsules by X-ray micro-tomography"*, Fusion Engineering and Design 75-79 (2005) 1005-1059.

[3] **Simon M., Sauerwein C., Tiseanu I., Burdairon S.**, *"Multi-purpose 3D computer tomography system"*, Proc. European Conference on Nondestructive Testing, Barcelona, Spain, June 17-21,2002

[4] **Hammersberg P., Mangard M.**, "*Correction for beam hardening artefacts in computerized tomography",* Journal of X-ray Science and Technology, 8-1 (1998) 5–93

[5] **Jennings R.J.**, "*A method for comparing beam hardening filter materials for diagnostic radiology*", Medical Physics, 15 (1988) 588–599.

[6] **Tiseanu I., Craciunescu T., Mandache N.B., Gherendi F.**, "*Microtomography analysis of fusion material samples",* EFDA TW5-TTMI-004: deliverable D6a, INTERIM REPORT, July 2004, EURATOM-MEdC Association

[7] **Fischer U., Simakov S.**, private communication.

[8] **Tiseanu I., Mandache N.B., Craciunescu T., Gherendi F.**, *"Non-destructive analysis of fusion materials samples by micro-tomography"*, EFDA TW0-TTMI-003: deliverable D3, FINAL REPORT.

Collaborative actions

3D X-RAY MICRO-TOMOGRAPHY FOR MODELING OF NB3SN MULTIFILAMENTARY SUPERCONDUCTING WIRES

I. Tiseanu, T. Craciunescu, T. Petrisor (MEdC),

A. della Corte (ENEA Frascati)

1. Introduction

Practical superconducting cables are composite wires consisting in superconducting filaments (d<10 μm) embedded in a normal-conducting matrix, usually Cu. Due to its excellent superconducting properties (TC=18 K and upper critical magnetic field BC2(4.2 K) = 23-29 T, depending on chemical composition, Nb3Sn is the most used low temperature superconducting material for the manufacturing of superconducting cable for large scale applications such as: energy transportation and storage (SMES-Superconducting Magnet Energy Storage), high field superconducting magnets (up to 20 T), NMR (Nuclear Magnetic Resonance) magnets, Superconducting Super Colider accelerator magnets, magnets for the fusion reactor, etc. In spite of the excellent superconducting properties, Nb3Sn is a brittle intermetallic compound and it cannot be processed by mechanical working (e.g drawing). Several techniques have been developed all using ductile precursor materials for composite wire processing. Essentially, Nb and Sn bars are embedded in a Cu matrix and- after drawing at the final diameter of the wire- the resulting composite, containing the micrometric filaments of Nb, is heat treated to form the Nb3Sn compound by diffusion. The concept of multifilamentary Nb3Sn wires is shown in Figure 1.

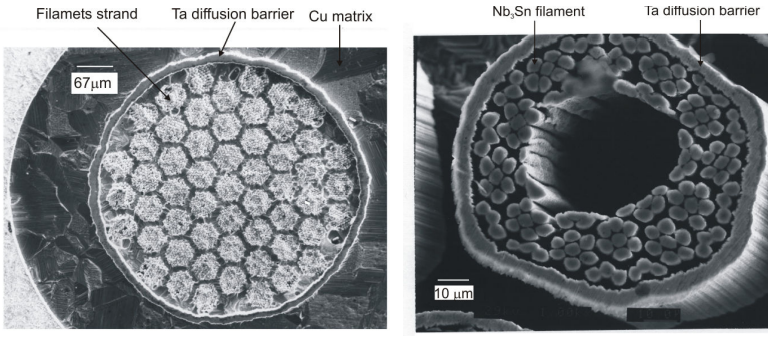

Figure1. Cross section of a Nb3Sn multifilamentary wire (left) and filaments strand within the wire (right)

2. Materials and method

Due to the fabrication process, multifilamentary Nb3Sn wires often exhibit an interfilament electrical contact and a concomitant increase in the magnetic hysteresis loss above that due to the intrinsic magnetic hysteresis of the filaments. For the in-situ processed Nb3Sn wire, the excess loss was attributed to the intermittent filament contact. The excess loss by eddy-current is very important when the filamentary conductors are exposed to changing fields. As it was demonstrated, a very simple technique to reduce the eddy-current losses is to twist the wire and the filaments during the manufacture. The twisting also reduces the time-independent proximity effect between the filaments and its associated loss. The twist-pitch parameter is defined as $\lambda = \pi D / \tan\phi$, were D is the wire diameter and ϕ is the angle between the filament and the wire axis. The λ is the main parameter which is taken into account in the theoretical models regarding the eddy-current losses and the critical current density (J_c) in the twisted Nb3Sn multifilamentary superconducting wire. Therefore, the measuring of the twist-pitch parameter is very important in order to compare the theoretical models with the experimantal transport and magnetic hysteresis data and, finally, for the modeling of the superconducting multifilamentary wire. At the time being, the only method for measuring the λ consists in etching the copper in a nitric acid solution, thus evidencing the twisted structure. The present method has two main drawbacks: it is distructive and does not permit the visualisation of the Nb3Sn filaments. The 3D X-ray would overcome these drawbacks. Moreover, it would permit the construction of the 3D image of the multifilamentary wire enabling us to determine the number of interfilament contacts on unite legth,ξ , as well as the twist-pitch parameter, λ. Thus, by taking into account both ξ and λ, a more complex model of the multifilamentary superconducting wire can be developed in order to explain the role of the internal wire structure on the superconducting transport properties.

An illustration of the application of the 3D microtomography technique is presented in Figure 2.

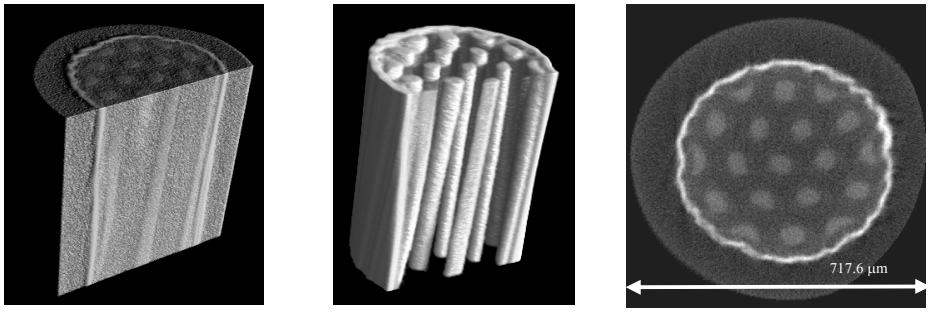

Figure 2. 3-D microtomography of Nb3Sn multifilamentary wire: 3-D reconstruction (top-left), 3-D reconstruction after thresholding (top-right), axial cross-section (bottom-left) and longitudinal cross-section (bottom-right)

The measurements were carried out in the X-ray Microtomography laboratory of NILPRP, [EFDA Newsletter, Vol 2003/2, and Vol 2003/6]. In these measurements we reached the outstanding resolution of 1.2 µm/ voxel.

3. Outlook

In the frame of this activity Nb3Sn multifilamentary wires for ITER (International Thermonuclear Experimental Reactor) will be studied. The ITER design criteria require 0,81 mm Nb3Sn wires with an overall critical current of at least 200 A (at 12 T and 4,2 K), equivalent with a non-Cu critical current density of 800 A/cm2, a Cu/non-Cu ratio of about 1 and hysteresis losses less than 1000 kJ/m3 for 3 T field cycle at 4.2 K. The role of this study is the modeling of the transport properties of the Nb3Sn wire in order to optimize the fabrication process in terms of the hysteresis losses, critical current and the Cu/non-Cu ratio.

METHOD AND DEVICE FOR THE NDT INSPECTION OF W COATING UNIFORMITY

I. Tiseanu, T. Craciunescu, , C. Ruset (MEdC),

H. Maier (Materialforschung Max-Planck-Institut für Plasmaphysik, Garching)

1. Principle of method

The thickness of CFC coating is determined by absorption contrast of transmitted X-rays. In order to mitigate the beam hardening (due to polychromatic character of the X-ray energy spectra) and scattering effects one recommends two X-ray transmission measurements: before and after coating. The useful result consists in subtraction of the two radiographies.

Additionally, the sample radiography is offset and gain corrected. Offset correction means the subtraction of the “dark” image (image without X-ray exposure). The gain correction

consists in the flattening of the detector response by a reference "white" image (image with X-ray exposure but without sample).

2. Coating uniformity inspection: example

In order to check the accuracy of the method, a non-uniform W coating was produced on a CFC tile and than inspected by X-Ray Radiography (XRR) technique. The results are shown in Figure1. The subtraction was performed after applying an image registration procedure for a perfect matching of the two radiographies (before and after coating). In this way, the CFC layer's fine structure do not creates artifacts in the final image. The gray values in the image are proportional to the coating thickness. The next profiles are along the colored horizontal lines. In this example the non-uniformity of the W layer is well within 4%.

The ratio between the maximum thickness (central area) and the thickness in the lateral areas was checked with another sample, which was cut and examined by metallographic technique. The values obtained by the two techniques were very similar.

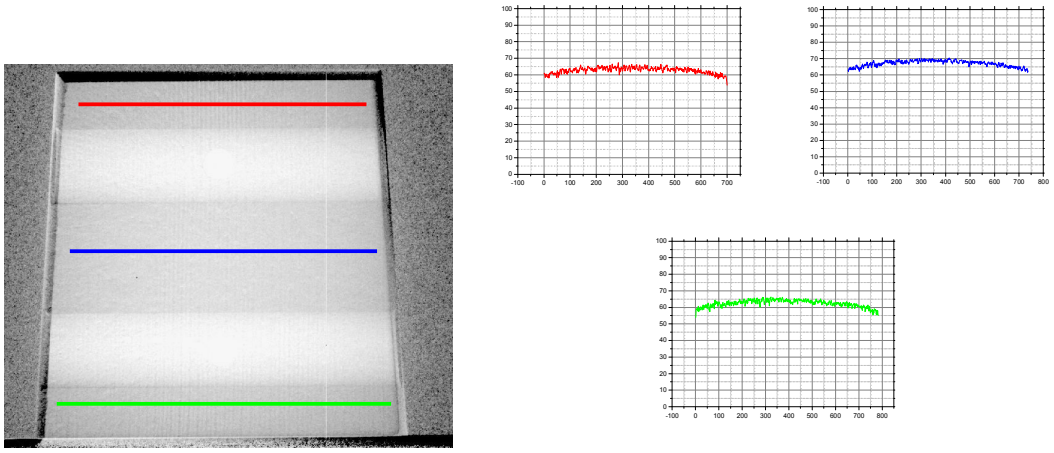

Figure 1. Results of the investigation of sample 135A. Profiles (along colored lines) showing the non-uniformity of the W layer.

3. Thickness of W coating determination

The capability to determine the thickness of the W coating (after calibration using an etalon sample) was demonstrated on samples provided by Materialforschung Max-Planck-Institut für Plasmaphysik. The samples are fine grain graphite SGL Carbon R6710, approx 50*50*20 mm³. Three parallel layers of W coating - 2.0, 2.1, and 2.2 μm - were realized by sputtering.

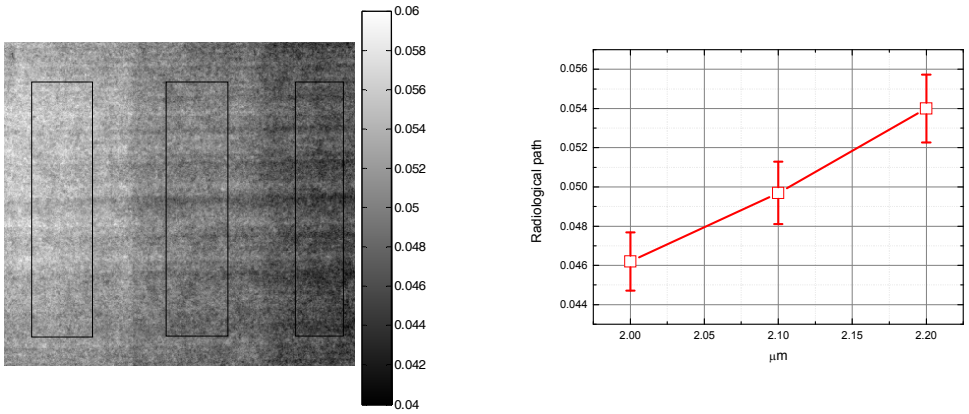

Figure 2. Analysis of the 3-layers coating sample: processed image I (left) and thickness evaluation (obtained after averaging three region of interest for the three thicknesses) (right)

Figure 2 presents the image $I = \log(I_{nd} - D) - \log(I_d - D)$, where I_{nd} is the radiographic image of the reference sample, I_d is the radiographic image of the coated sample and D is the image obtained without X-rays (detector intrinsic background). Three regions of interests (ROI) were defined, corresponding to the three coating thickness. The dependence of the average value of the radiological path for the three ROIs on the coating thickness demonstrates that the absolute errors in thickness are about 3%.

4. Outlook

The methods developed and the experiments performed demonstrate the usefulness of X-ray techniques in coating uniformity and coating thickness determination.

Currently, we are developing multi-energy digital radiography techniques in order to determine the absolute coating thickness independent of substrate samples. We believe that a robust non-invasive technique for the diagnostics of thin deposited layers is of growing interest in the current and future fusion technology.